SUPERSONIC LAMINAR FLOW REATTACHMENT AND REDEVELOPMENT BEHIND A TWO-DIMENSIONAL REARWARD FACING STEP

Donald J. Spring

Army Missile Command
Redstone Arsenal, Alabama

31 October 1972

AD

TECHNICAL REPORT
RD-72-16

SUPERSONIC LAMINAR FLOW REATTACHMENT AND REDEVELOPMENT BEHIND A TWO-DIMENSIONAL REARWARD FACING STEP

by

Donald J. Spring

October 1972

U.S. ARMY MISSILE COMMAND
Redstone Arsenal, Alabama

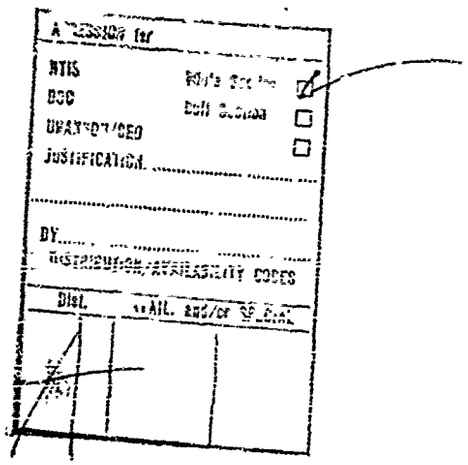

DISPOSITION INSTRUCTIONS

DESTROY THIS REPORT WHEN IT IS NO LONGER NEEDED. DO NOT RETURN IT TO THE ORIGINATOR.

DISCLAIMER

THE FINDINGS IN THIS REPORT ARE NOT TO BE CONSTRUED AS AN OFFICIAL DEPARTMENT OF THE ARMY POSITION UNLESS SO DESIGNATED BY OTHER AUTHORIZED DOCUMENTS.

TRADE NAMES

USE OF TRADE NAMES OR MANUFACTURERS IN THIS REPORT DOES NOT CONSTITUTE AN OFFICIAL INDORSEMENT OR APPROVAL OF THE USE OF SUCH COMMERCIAL HARDWARE OR SOFTWARE.

DOCUMENT CONTROL DATA - R & D

(Security classification of title, body of abstract and indexing annotation must be entered when the overall report is classified)

1. ORIGINATING ACTIVITY (Corporate author) Aeroballistics Directorate US Army Missile Res, Dev & Eng Lab US Army Missile Command Redstone Arsenal, Alabama 35809	2a. REPORT SECURITY CLASSIFICATION UNCLASSIFIED 2b. GROUP NA

3. REPORT TITLE

SUPERSONIC LAMINAR FLOW REATTACHMENT AND REDEVELOPMENT BEHIND A TWO-DIMENSIONAL REARWARD FACING STEP

4. DESCRIPTIVE NOTES (Type of report and inclusive dates)

Technical Report

5. AUTHOR(S) (First name, middle initial, last name)

Donald J. Spring

6. REPORT DATE 31 October 1972	7a. TOTAL NO. OF PAGES 48 51	7b. NO. OF REFS 27
8a. CONTRACT OR GRANT NO. b. PROJECT NO. NA c. d.	9a. ORIGINATOR'S REPORT NUMBER(S) RD-72-16 9b. OTHER REPORT NO(S) (Any other numbers that may be assigned this report) AD_____	

10. DISTRIBUTION STATEMENT

Approved for public release; distribution unlimited.

11. SUPPLEMENTARY NOTES None.	12. SPONSORING MILITARY ACTIVITY Same as No. 1.

13. ABSTRACT

A theoretical study of the flow recompression, reattachment, and redevelopment associated with a supersonic laminar isoenergetic flow past a back step was made. Based on an integral approach, the governing system of ordinary differential equations for such recompression and redevelopment processes was derived by introducing simplified flow models. The preceding constant pressure jet mixing region was analyzed so as to provide the necessary initial conditions for the recompression process. The effect of finite initial boundary layer on this mixing process was also taken into account. The system of equations for recompression was integrated with the base pressure and the starting location of recompression as parameters. These parameters were then determined through the conditions to be satisfied at the point of reattachment. The calculated base pressure ratios agreed well with the experimental data. Some analysis was continued for the flow redevelopment downstream of reattachment. With slight modification of the results at the point of reattachment, the pressure distribution within the redeveloping flow region can be predicted fairly well for the flow case of $M_1 = 2.0$. Additional possible improvements to the analysis was suggested and discussed.

4. KEY WORDS	LINK A		LINK B		LINK C	
	ROLE	WT	ROLE	WT	ROLE	WT
Recompression and redevelopment processes						
Simplified flow models						
Upper viscous layer						
Wake flow region						
Laminar mixing analysis						
Calculation procedures						

31 October 1972

Technical Report RD-72-16

SUPERSONIC LAMINAR FLOW REATTACHMENT AND REDEVELOPMENT BEHIND A TWO-DIMENSIONAL REARWARD FACING STEP

by

Donald J. Spring

Approved for public release; distribution unlimited.

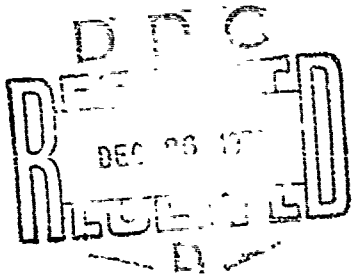

Aeroballistics Directorate
US Army Missile Research, Development and Engineering Laboratory
US Army Missile Command
Redstone Arsenal, Alabama 35809

IC

CONTENTS

NOMENCLATURE

C	$(\rho u/\rho_e u_e)$, Chapman-Rubesin parameter
c	V/V_{max}, Crocco number
F*	Normalized shear function
H	Step height
h_b	Height for back flow
ℓ_m	Length of the constant pressure region along the wake boundary measured from the separation corner
ℓ_{w_k}	$H/\sin \theta_\infty$, length of the wake boundary measured from the separation corner to the point of reattachment
M	Mach number
p	Pressure
R	Specific gas constant
R_e	U_∞/ν_∞, Reynolds number
r	Location of the reattachment point measured from the base of the step
S*	Streamwise distance function defined by Eq. (2.29)
T	Temperature
u	x-velocity component
V	Magnitude of velocity
v	y-velocity component
x	Coordinate in main flow direction
y	Coordinate normal to x
α	u_∞/u_R, reference perturbation velocity
β	Streamline angle

γ	Ratio of specific heat
δ	Thickness of viscous layer
ζ	y/δ_a or y/δ_b
η	$\sigma_L y/x$, mixing ordinate
θ	Angle or momentum thickness
μ	Viscosity
ν	Kinematic viscosity
ρ	Density
σ_L	Laminar spread rate parameter
τ	Shear stress
φ	u/u_e, dimensionless velocity
$\omega(c)$	Prandtl-Meyer function

Subscripts

a	Viscous layer above the dividing streamline
b	Viscous layer below the dividing streamline
d	Dividing streamline
e	External inviscid stream
ℓ	Characteristic length for Reynolds number measured from leading edge of plate to separation point
w	Wall
0	Stagnation state
1	Approaching flow state, or initial control volume station
2	Flow state after the Prandtl-Meyer expansion, or final control volume station
∞	Station at the beginning of recompression

1. INTRODUCTION

One of the problems facing designers of flight vehicles with relatively blunt bases has been the accurate prediction of the base pressure acting upon the body base. For certain configurations and flight conditions the resulting base drag makes a significant contribution (as much as one-third) to the overall drag of the vehicle. Recognition of this problem has led to a considerable amount of research over the last quarter of a century in an attempt to reach a better understanding of the flow field.

It was recognized early that, for a flow past a blunt base or step (see Fig. 1), the flow is unable to follow the body contour, thereby resulting in a separation of the flow. For supersonic approaching flows, it will expand from the initial pressure to that of the base pressure at the corner. At the same time, the boundary layer will also follow this expansion process. As a result of the separation, the free shear layer is energized by a mixing process and prepares itself for the subsequent reattachment. The interaction between the inviscid and viscid stream controls and determines the overall flow field. For practical purposes, the pressure in the initial part of the mixing region is constant; however, close to the recompression region, this simplification is not justified since appreciable pressure rises have been observed along the flow. In addition, considerable variation of static pressure exists across the flow as a result of the finite

curvature of the streamlines. Little effort has been expended in understanding the flow field in the region of recompression or reattachment.

Early researchers [1, 2, 3] developed empirical methods to predict the base pressure which was found as only a function of free-stream Mach number and it was not until the early work of Chapman [4] that the importance of Reynolds number effects was recognized. Chapman proceeded to formulate a semiempirical method and showed the dependency of base pressure upon Mach number and characteristic Reynolds number. Further extensions of these ideas were proposed by Love [5]. These semiempirical methods, while giving quick estimations of base pressures, were unable to describe the mechanics of the flow field.

The first attempt to qualitatively explain the complex flow field appears to have been accomplished by Crocco and Lees [6]. They used an integral approach where the momentum transfer across the mixing region was estimated by a proper average constant rate. The wake region is thus energized until it can support the recompression process as the flow returns to the direction of the original flow. Chapman [7] suggested the concept which presently is the basis for most of the component approaches to the base pressure problem. He visualized a region at the base of the body commonly referred to as the "dead-air" region which was responsible for maintaining equilibrium in the flow and, thus, the concept of a dividing streamline was born. Korst [8] adapted the dividing streamline concept in a base pressure

theory. This approach is commonly referred to as the Chapman-Korst model. The equilibrium condition states that the total pressure along the dividing streamline must possess only enough mechanical energy to support the recompression process up to the rear stagnation point. The fluid beneath the dividing streamline is returned and conserved within the wake while that above the dividing streamline continues downstream. Korst used an eddy-viscosity concept to solve several cases of turbulent mixing while Chapman [9] used a similarity solution for laminar mixing. Both methods assumed that the pressure at reattachment could be determined from isentropic relationships.

Following these efforts Lees et al [10, 11] extended the Crocco-Lees method by developing a technique that eliminated the experimentally determined mixing coefficient by introducing the first moment of momentum equation. They showed that a throat or critical point existed in the flow downstream of the reattachment point. The base pressure was determined by the requirement that the flow pass smoothly through this throat. Alber and Lees [12] later extended the integral viscid-inviscid theory to turbulent flows. A turbulent eddy-viscosity model was formulated from that of an incompressible flow by adopting a certain reference density. However, in all of the preceding case, no detailed studies of the recompression process were completed. Most of the other methods used empirical corrections based upon experimental data such as that proposed by Nash [13] to accurately predict the reattachment pressure.

Later efforts directed to solving the wake problem have included the method of integral relations as applied by Crawford [14] and numerical solutions to the Navier-Stokes equations [15]. In addition

to these methods, Weiss and Weinbaum [16, 17, 18, 19] obtained detailed solutions of the near wake by dividing the flow field into three regions. Each region is solved using a different technique, hence, their methods are commonly referred to as multimethod base flow theories. The rotational outer flow resulting from the expansion of the boundary layer is solved using the method of characteristics, the viscous layer above the dividing streamline is treated using a modified Oseen solution of the boundary layer equations, and the recirculation region is solved by a finite-difference representation of the full Navier-Stokes equations. Coupling is assured by requiring continuity of flow properties on the dividing streamline. The disadvantage to this last group of methods is that even with the advent of high speed computers a considerable amount of computational time is required to study each case.

Chow [20] in 1970 developed a technique to study the turbulent reattachment which yields satisfactory results for the recompression pressure distribution up to the reattachment point without the extensive use of empirical information. A constant pressure turbulent jet mixing precedes the recompression region where due to the turning process the normal pressure gradient can no longer be neglected. By developing a system of equations which also must be satisfied at the reattachment point, a solution can be obtained.

The present effort is an examination of the reattachment process within the two-dimensional laminar flow regime. By following, in general, the approach as suggested by Chow for turbulent flow, it is felt that laminar flow cases can be studied in more detail since many factors which influence the recompression processes and had to be

ignored in turbulent flow studies, can be investigated and explored. In addition, the study of flow redevelopment and rehabilitation after reattachment which can not be adequately handled in turbulent flows would fully illustrate the behavior of relaxation toward the equilibrium flow far downstream. Isoenergetic flow shall be assumed throughout this analysis and, thus, the energy consideration is conveniently eliminated.

2. DEVELOPMENT OF ANALYTICAL EQUATIONS

2.1 General Considerations

It is expected that the boundary layer concepts still give a valid description of the flow for the present problem. However, it is also recognized that within the region of recompression and redevelopment, the curvature of the streamlines is not negligible; i.e., the simplification of $\partial p/\partial y = 0$ across the viscous region can no longer be adopted. Integral analysis was employed to solve the governing system of equations derived for the viscous layers incorporating their interaction with the outer free stream. The requirement that the same flow properties, along the common boundary joining the upper and lower viscous layers, determines a proper solution.

2.2 Formulation of the Jet Reattachment Process

The recompression region shown in Fig. 2 is divided into two parts along the dividing streamline. Fluid contained within the region above the dividing streamline will proceed downstream while that below the dividing streamline will be turned back into the wake region. The upper shear layer interacts with the external flow which guides and receives the influence of the shear layer by following an inverse Prandtl-Meyer relationship. One can describe the interaction from the fact that the transverse velocity component at the edge of the shear layer induces an increase in pressure in the outer free stream which in turn exerts an influence on the flow properties within the layer

including this transverse velocity component at the edge of the shear layer itself.

2.2.1 Upper Viscous Layer

Conservation of mass across the upper shear layer (see Fig. 3) requires

$$\frac{\partial}{\partial x}(\rho u) + \frac{\partial}{\partial y}(\rho v) = 0 \quad . \tag{2.1}$$

Choosing an x-coordinate to be coincident with the dividing streamline, one can integrate Eq. (2.1) across the shear layer to obtain

$$-\rho_e v_e = \int_0^{\delta_a} \frac{\partial}{\partial x}(\rho u)\, dy \quad .$$

Upon employing Leibnitz's Rule, the above equation can be rewritten as

$$-\rho_e v_e = \frac{d}{dx}\int_0^{\delta_a} \rho u\, dy - \rho_e u_e \frac{d\delta_a}{dx}$$

After nondimensionalizing with the free-stream properties and after some manipulations, one obtains the streamline angle at the edge of the upper shear layer as given by

$$\tan \beta_e = \frac{v_e}{u_e} = \frac{d}{dx}\left[\delta_a \int_0^1 \left(1 - \frac{\rho}{\rho_e}\varphi\right) d\zeta\right]$$

$$- \frac{\delta_a \int_0^1 \frac{\rho}{\rho_e}\varphi\, d\zeta}{\left(1 - c_e^2\right)^{\frac{1}{(\gamma-1)}} c_e} \frac{d}{dx}\left[\left(1 - c_e^2\right)^{\frac{1}{(\gamma-1)}} c_e\right] \quad , \tag{2.2}$$

where

$$c_e = \frac{V_e}{V_{max}} \simeq \frac{u_e}{V_{max}} \; ; \quad \bar{\varphi} = \frac{u}{u_e} \; ; \quad \zeta = \frac{y}{\delta_a} \quad .$$

Since the free-stream follows the Prandtl-Meyer relationship, the streamline angle β_e is related to the Prandtl-Meyer function ω by

$$\beta_e = \beta_\infty + \omega(c_\infty) - \omega(c_e) \quad , \tag{2.3}$$

where β_∞ is the difference between the dividing streamline angle and the free-stream angle within the upstream constant pressure jet mixing region.

Referring to the elementary control volume as depicted in Fig. 4, application of the principle of momentum conservation for the upper shear layer gives

$$\left[\frac{d}{dx}\int_0^{\delta_a} \rho u^2\, dy - u_e \frac{d}{dx}\int_0^{\delta_a} \rho u\, dy\right] dx = \int_0^{\delta_a} p\, dy + p_e\, d\delta_a$$

$$- \int_0^{\delta_a} p\, dy - \frac{d}{dx}\int_0^{\delta_a} p\, dy\, dx - \tau_d\, dx \quad . \tag{2.4}$$

Upon rearranging, Eq. (2.4) can be rewritten as

$$\frac{d}{dx}\int_0^{\delta_a} \rho u(u_e - u)\, dy - \int_0^{\delta_a} \rho u\, dy\, \frac{du_e}{dx} + p_e \frac{d\delta_a}{dx} - \frac{d}{dx}\int_0^{\delta_a} p\, dy = \tau_d$$

or

$$\frac{d}{dx}\left[\rho_e u_e^2 \delta_a \int_0^1 \frac{\rho}{\rho_e}\varphi(1-\varphi)\,d\zeta\right] - \rho_e u_e \frac{du_e}{dx}\delta_a \int_0^1 \frac{\rho}{\rho_e}\varphi\,d\zeta$$

$$+ p_e \frac{d\delta_a}{dx} - \frac{d}{dx} p_e \delta_a \int_0^1 \frac{p}{p_e}\,dy = \tau_d \quad . \tag{2.5}$$

From additional manipulation of the last two terms on the left-hand side of Eq. (2.5), one may write

$$p_e \frac{d\delta}{dx} - \frac{d}{dx}\left(p_e \delta \int_0^1 \frac{p}{p_e}\,dy - 1 + 1\right) = \delta_a \frac{dp_e}{dx} - \frac{d}{dx}\left[p_e \delta_a \int_0^1 \left(\frac{p}{p_e} - 1\right) d\zeta\right]$$

$$= \rho_e u_e \delta_a \frac{du_e}{dx} - \frac{d}{dx}\left[p_e \delta_a \int_0^1 \left(\frac{p}{p_e} - 1\right) d\zeta\right] \quad .$$

Thus, Eq. (2.5) becomes

$$\frac{d}{dx}\left[\rho_e u_e^2 \delta_a \int_0^1 \frac{\rho}{\rho_e}\varphi(1-\varphi)\,d\zeta\right] + \rho_e u_e \delta_a \left[1 - \int_0^1 \frac{\rho}{\rho_e}\varphi\,d\zeta\right]\frac{du_e}{dx}$$

$$- \frac{d}{dx}\left[p_e \delta_a \int_0^1 \left(\frac{p}{p_e} - 1\right) d\zeta\right] = \tau_d \quad . \tag{2.6}$$

For simplification, one may assume

$$\frac{p}{p_e} = \frac{p_d}{p_e} - \frac{3}{2}\left(\frac{p_d}{p_e} - 1\right)\zeta + \frac{1}{2}\left(\frac{p_d}{p_e} - 1\right)\zeta^3$$

for the pressure variation across the upper viscous layer, which satisfies the boundary conditions

$$\text{at } \zeta = 0 \qquad p = p_d$$

$$\text{at } \zeta = 1 \qquad p = p_e; \quad \frac{\partial\left(\frac{p}{p_e}\right)}{\partial \zeta} = 0 \quad .$$

Eq. (2.6) can now be written as

$$\frac{d}{dx}\left[\left(1 - c_e^2\right)^{\frac{1}{\gamma - 1}} c_e^2 \delta_a \int_0^1 \frac{\rho}{\rho_e} \varphi(1 - \varphi)\, d\zeta\right] + \left(1 - c_e^2\right) c_e \delta_a \left[\int_0^1 \left(1 - \frac{\rho}{\rho_e}\varphi\right) d\zeta\right] \frac{dc_e}{dx}$$

$$- \frac{3}{16}\left(\frac{\gamma - 1}{\gamma}\right) \frac{d}{dx}\left[\left(1 - c_e^2\right)^{\frac{\gamma}{\gamma - 1}} \delta_a \left(\frac{p_d}{p_e} - 1\right)\right] = \frac{\tau_d}{\rho_\infty u_\infty^2} \left(1 - c_\infty^2\right)^{\frac{1}{\gamma - 1}} c_\infty^2 \quad . \tag{2.7}$$

For this upper shear layer, a velocity profile of third-order polynomials is assumed, i.e.,

$$\varphi = \varphi_d + \left.\frac{\partial \varphi}{\partial \zeta}\right|_d \zeta + \left[3\left(1 - \varphi_d\right) - 2 \left.\frac{\partial \varphi}{\partial \zeta}\right|_d\right] \zeta^2 + \left[\left.\frac{\partial \varphi}{\partial \zeta}\right|_d - 2\left(1 - \varphi_d\right)\right] \zeta^3 \quad , \tag{2.8}$$

which satisfies the boundary conditions

$$\varphi = \varphi_d \; ; \quad \frac{\partial \varphi}{\partial \zeta} = \left.\frac{\partial \varphi}{\partial \zeta}\right|_d \quad \text{at } \zeta = 0 \quad ,$$

and

$$\varphi = 1 \; ; \quad \frac{\partial \varphi}{\partial \zeta} = 0 \quad \text{at } \zeta = 1 \quad .$$

It is recognized that at the rear stagnation point ($\varphi_d = 0$), the velocity and the stress should vanish so that a simple correlation between the slope parameter $(\partial\varphi/\partial\zeta)_d$ and φ_d would be that they are linearly proportional to each other, with the constant of proportionality being evaluated from initial conditions prevailing at the end of the mixing region.

The expression for the pressure difference across the upper layer can be obtained from vertical momentum considerations. The basic equation is given by

$$\frac{\partial}{\partial x}(\rho uv) + \frac{\partial}{\partial y}\left(\rho v^2\right) = -\frac{\partial p}{\partial y} + \frac{\partial \tau_{xy}}{\partial x} \quad . \tag{2.9}$$

Integrating across the upper layer one obtains

$$\frac{d}{dx}\left[\rho_e u_e^2 \delta_a \int_0^1 \frac{\rho}{\rho_e} \varphi^2 \tan\beta \, d\zeta\right] - \rho_e u_e v_e \frac{d\delta_a}{dx} + \rho_e u_e^2 \tan^2 \beta_e$$

$$= \left(p_d - p_e\right) + \frac{d}{dx}\int_0^{\delta} \rho v \, du \quad , \tag{2.10}$$

with $\tan\beta = \tan\beta_e\left(2\zeta - \zeta^2\right)$.

The shear stress in Eq. (2.9) has been evaluated from

$$\tau_{xy} = \mu \frac{\partial u}{\partial y}$$

where μ is the viscosity which is assumed to be linearly proportional to temperature. Upon rearranging and normalizing, Eq. (2.10) yields the final expression for the pressure difference across the upper layer, i.e.,

$$\left(\frac{p_d}{p_e} - 1\right) = \frac{2\gamma}{\gamma - 1}\left\{\frac{c_e^2}{1 - c_e^2}\left(\tan^2\beta_e - \tan\beta_e \frac{d\delta_a}{dx}\right) + \frac{1}{\left(1 - c_e^2\right)^{\frac{\gamma}{(\gamma-1)}}}\right.$$

$$\left.\frac{d}{dx}\left[\left(1 - c_e^2\right)^{\frac{1}{\gamma-1}} c_e^2 \left(\delta_a \int_0^1 \frac{\rho}{\rho_e}\varphi^2 \tan\beta \, d\zeta - \frac{\nu}{u_e}\int_{\varphi_d}^1 \frac{\rho}{\rho_e} \, d\varphi\right)\right]\right\} \quad . \tag{2.11}$$

2.2.2 Wake Flow Region

The lower wake region consists of two subregions separated by a line of zero longitudinal velocity as shown in Fig. 5. The upper subregion consists of a flow characterized by the dividing streamline velocity and the lower subregion represented by a back flow velocity. A linear velocity profile is assumed for the upper layer while a cosine profile is assumed for the back flow.*

The mass flow in the upper subregion is

$$\int_0^{\delta_b} \rho u dy = \rho_d u_d \delta_b \left(1 - c_d^2\right) \int_0^1 \frac{\zeta}{\left(1 - c_d^2 \zeta^2\right)} d\zeta$$

which after carrying out the integration for isoenergetic flows gives,

$$\int_0^{\delta_b} \rho u dy = \sqrt{\frac{2\gamma}{R(\gamma - 1)\, T_0}}\, \frac{p_d \delta_d}{2c_d} \left[-\ell n\left(1 - c_d^2\right)\right] . \qquad (2.12)$$

For the back flow,

$$\int_0^{h_b} \rho u dy = \rho_b u_b h_b \int_0^1 \frac{\rho}{\rho_b} \frac{u}{u_b} d\zeta$$

or

$$\int_0^{h_b} \rho u dy = \frac{2}{\pi} \rho_b u_b h_b \left(1 - c_b^2\right) \int_0^{\frac{\pi}{2}} \frac{\cos \zeta \, d\zeta}{1 - c_b^2 \cos^2 \zeta}$$

The above expression may be integrated directly to yield

*Accounting for the wall boundary layer does not change the basic equations for the same assumed profile.

$$\int_0^{h_b} \rho u dy = \sqrt{\frac{2\gamma}{R(\gamma - 1)\, T_0}}\ \frac{\rho_b^{\,2}\, h_b}{\pi\sqrt{1 - c_b^2}}\ \tan^{-1}\ \frac{c_b}{\sqrt{1 - c_b^2}} \quad . \quad (2.13)$$

From Eqs. (2.12) and (2.13), the mass balance for the wake region imposes a condition that

$$\frac{\delta_b}{h_b} = \frac{\frac{4}{\pi}\frac{p_w}{p_d}\ \frac{c_d}{\sqrt{1 - c_d^2}}\ \tan^{-1}\ \frac{c_b}{\sqrt{1 - c_b^2}}}{-\ell n\left(1 - c_d^2\right)} \quad . \quad (2.14)$$

In addition, if a straight line trajectory is assumed for the dividing streamline, the geometry of the wake gives the following relationships:

$$\frac{\delta_b}{\delta_{b_\infty}} = \frac{\ell_{w_k} - \left(\ell_m + x\right)}{\ell_{w_k} - \ell_m} \quad (2.15)$$

and

$$\frac{\delta_b}{h_b} = \frac{\sin \theta_d}{\sin\left(\theta_\infty - \theta_d\right)} \quad . \quad (2.16)$$

The difference in pressure across the wake flow may be calculated by using vertical momentum considerations. The control volume used for this analysis is shown in Fig. 6. For simplification, it is assumed that the forward flow has the constant pressure p_d of the dividing streamline while the back flow has the constant wall pressure p_w. It is expected that the normal momentum fluxes associated with the transverse velocity component are small and tend to cancel each other. Thus, they are neglected in this analysis. One now obtains

$$\left(p_w - p_d\right) dx_w - \tau_d \sin \theta_\infty \, dx = - \frac{d}{dx} \int_0^{\delta_b} \rho u^2 \sin \theta_\infty \, dy \, dx \quad ,$$

which is equivalent to

$$\frac{p_w}{p_d} \frac{p_d}{p_e} \frac{p_e}{p_{0_\infty}} = \frac{p_d}{p_e} \frac{p_e}{p_{0_\infty}} + \frac{\tau_d}{\rho_\infty u_\infty^2} \left(1 - c_\infty^2\right)^{\frac{1}{\gamma - 1}} c_\infty^2 \frac{2\gamma}{\gamma - 1} \left(\frac{\sin \theta_\infty \cos \theta_d}{\cos\left(\theta_\infty - \theta_d\right)} \right)$$

$$+ \frac{d}{dx} \left[\frac{p_d}{\rho_{0_\infty}} u_d^2 \sin \theta_\infty \, \delta_b \int_0^1 \frac{\rho}{\rho_e} \varphi^2 d\zeta \right] \quad . \tag{2.17}$$

Upon integrating and rearranging, Eq. (2.17) becomes

$$\frac{p_w}{p_d} = 1 + \frac{2\gamma}{\gamma - 1} \frac{\sin \theta_\infty}{\left(\frac{p_d}{p_e}\right)\left(\frac{p_e}{p_{0_\infty}}\right)} \left\{ \frac{\cos \theta_d}{\cos\left(\theta_\infty - \theta_d\right)} \frac{\tau_d}{\rho_\infty u_\infty^2} \left(1 - c_\infty^2\right)^{\frac{1}{\gamma - 1}} c_\infty^2 \right.$$

$$\left. - \frac{d}{dx_w} \left[\frac{p_d}{p_e} \frac{p_e}{p_{0_\infty}} \delta_b \left(\frac{1}{2 c_d} \ell n \frac{1 + c_d}{1 - c_d} - 1 \right) \right] \right\} \quad . \tag{2.18}$$

We now consider the momentum relationship associated with the wake flow. The momentum associated with the upper subregion is

$$\int_0^{\delta_b} \rho u^2 dy = \rho_d u_d^2 \delta_b \left(1 - c_d^2\right) \int_0^1 \frac{\zeta^2}{1 - c_d^2 \zeta^2} \, d\zeta \quad ,$$

which after integration gives

$$\int_0^{\delta_b} \rho u^2 dy = \frac{2\gamma}{\gamma - 1} p_d \delta_b \left[\frac{1}{2 c_d} \ell n \frac{1 + c_d}{1 - c_d} - 1 \right] \quad . \tag{2.19}$$

For the lower subregion, the momentum associated with the cosine profile is

$$\int_0^{h_b} \rho u^2 dy = \rho_b u_b^2 h_b \int_0^1 \frac{\rho}{\rho_b} \varphi^2 d\zeta = \rho_b u_b^2 h_b \left(1 - c_b^2\right) \int_0^1 \frac{\cos^2 \frac{\pi}{2}\zeta \, d\zeta}{1 - c_b^2 \cos^2 \frac{\pi}{2}\zeta} \, . \tag{2.20}$$

After some algebraic manipulation, Eq. (2.20) becomes

$$\int_0^{h_b} \rho u^2 dy = \frac{2 h_b}{\pi} \frac{\left(1 - c_b^2\right)}{c_b^2} \rho_b u_b^2 \left[\frac{1}{2} \int_0^{\frac{\pi}{2}} \left(\frac{1}{1 - c_b \cos \frac{\pi}{2}\zeta} + \frac{1}{1 + c_b \cos \frac{\pi}{2}\zeta} \right) d\zeta - \frac{\pi}{2} \right]$$

and

$$\int_0^{h_b} \rho u^2 dy = \frac{h_b \left(1 - c_b^2\right)}{c_b^2} \rho_b u_b \left(\frac{1}{\sqrt{1 - c_b^2}} - 1 \right) \, . \tag{2.21}$$

The entire wake momentum balance is given by

$$p_d \delta_b - \left(p_d \delta_b - \frac{d}{dx} p_d \delta_b d_x \right) + \left[p_w h_b - \left(p_w h_b + \frac{d}{dx} p_w h_b d_x \right) \right] \cos \theta_\infty$$

$$+ \tau_d d_x - p_w dx_w \sin \theta_\infty = \frac{d}{dx} \int_0^{\delta_b} \rho u^2 dy \, dx + \frac{d}{dx} \int_0^{h_b} \rho u^2 dy \, dx \cos \theta_\infty$$

or

$$\tau dx = \left(p_d\delta_b + \int_0^{\delta} \rho u^2 dy\right)_1 - \left(p_d\delta_b + \int_0^{\delta_b} \rho u^2 dy\right)_2$$

$$+\left(p_w h_b + \int_0^{h} \rho u^2 dy\right)_1 \cos\theta_\infty - \left(p_w h_b + \int_0^{h_b} \rho u^2 dy\right)_2 \cos\theta_\infty$$

$$- p_w dx_w \sin\theta_\infty \quad . \tag{2.22}$$

After additional rearranging and substitution of relationship for dx_w/dx, we obtain

$$\tau_d = \frac{d}{dx}\left(p_d\delta_b + p_w h_b \cos\theta_\infty\right) + \frac{d}{dx}\left(\int_0^{\delta_b} \rho u^2 dy + \cos\theta_\infty \int_0^{h_b} \rho u^2 dy\right)$$

$$+ p_w \sin\theta_\infty \frac{dx_w}{dx} \quad .$$

Using Eqs. (2.19) and (2.21) and normalizing, the above equation becomes

$$\frac{\tau_d}{\rho_\infty u_\infty^2}\left(1 - c_\infty^2\right)^{\frac{1}{\gamma-1}} c_\infty^2 = \frac{\gamma-1}{2\gamma}\left\{\frac{d}{dx}\left[\frac{p_d}{p_e}\frac{p_e}{p_{0_\infty}}\left(\delta_b + \frac{p_w}{p_d} h_b \cos\theta_\infty\right)\right]\right.$$

$$\left. + \frac{p_w}{p_d}\frac{p_d}{p_e}\frac{p_e}{p_{0_\infty}} \frac{\sin\theta_\infty \cos\left(\theta_\infty - \theta_d\right)}{\cos\theta_d}\right\} + \frac{d}{dx}\left[\frac{p_d}{p_e}\frac{p_e}{p_{0_\infty}} \delta_b\left(\frac{1}{2c_d} \ln\frac{1 + c_d}{1 - c_d} - 1\right)\right.$$

$$\left. + \frac{p_w}{p_d}\frac{p_d}{p_e}\frac{p_e}{p_{0_\infty}} h_b \cos\theta_\infty\left(\frac{1}{\sqrt{1 - c_b^2}} - 1\right)\right] \quad . \tag{2.23}$$

The shear stress in Eqs. (2.7) and (2.23) is evaluated from

$$\tau_d = \nu\rho \left.\frac{\partial u}{\partial y}\right|_d = \frac{\nu}{u_e}\frac{\rho}{\rho_e} u_e \rho_e \frac{u_e}{\delta_a}\left.\frac{d\varphi}{d\zeta}\right|_d \quad , \tag{2.24}$$

which can be rearranged into

$$\frac{\tau_d}{\rho_\infty u_\infty^2}\left(1 - c_\infty^2\right)^{\frac{1}{\gamma-1}} c_\infty^2 = \frac{\nu}{u_e \delta_a}\left(1 - c_e^2\right)^{\frac{1}{\gamma-1}} c_e^2 \frac{\rho}{\rho_e}\left|_d \left.\frac{d\varphi}{d\zeta}\right|_d \right. \quad . \tag{2.25}$$

The initial conditions for this recompressive flow are provided for from the upstream constant pressure mixing region. In order to achieve a smooth joining between the mixing region and the recompression region, a constant pressure laminar mixing analysis was performed by assuming a velocity profile which was compatible with that assumed for the reattachment study.

2.2.3 Laminar Mixing Analysis

The laminar mixing analysis used is compatible with the reattachment analysis but applies to the case of isoenergetic flow only. The following formulation is applicable for the flow with a finite initial boundary layer thickness.

Chapman [9] has shown from a rigorous analysis that the nondimensional mixing ordinate for similar laminar flow can be represented by

$$\eta = \frac{\sqrt{R_{e_x}}}{x\sqrt{2}} \int \frac{\rho}{\rho_\infty}\, dy \quad . \tag{2.26}$$

From the differential equation for the mixing profile,

$$f''' + ff'' = 0 \quad . \tag{2.27}$$

Chapman obtained the solutions

$$\varphi_d = f'(0) = 0.5873$$

and

$$\left.\frac{\partial \varphi}{\partial \eta}\right|_0 = f''(0) = 0.2811 \quad .$$

These equations and solutions were developed by assuming that the viscosity was a function of temperature only and additionally that no inicial boundary layer thickness was present. This yields a single-valued solution for the dividing streamline velocity of 0.5873. Further research has shown that this solution is valid, however, only for large distance ($x \gg 1$) downstream of the separation point, which is not the case for realistic base flow problems. Additionally, one recognizes that there must be some rotational effects when the flow field interacts with the upper shear layer.

One could consider the rotational flow field by using the method of characteristics but this complicates the analysis and destroys the simplicity of a short engineering approach. Dennison and Baum [21] postulated a method for determining the dividing streamline velocity with an initial boundary layer thickness. They uncoupled the momentum equation from the energy equation for a finite initial profile in a laminar free shear layer. They solved the resulting equation for velocity and shear profiles using an implicit finite difference technique. The initial profile as the flow separates, corresponds to the Blasius profile in transformed coordinates. Initially, a Howarth transformation was used to reduce the equations to the incompressible form and for convenience of calculation another transformation to the

Crocco coordinate system was made. After considerable effort, they arrived at an equation for the nonfully developed dividing streamline velocity which is given as follows:

$$\varphi_d \frac{d\varphi_d}{dS^*} = F_d^* \left.\frac{\partial F^*}{\partial \varphi}\right|_d \quad , \tag{2.28}$$

where F* represents a normalized shear function and S* represents a streamwise distance function. The latter function can be defined as

$$S^* = CF_w^* \int_0^x \rho_e u_e u_e dx \quad , \tag{2.29}$$

where C is the Chapman-Rubesin parameter ($\rho u/\rho_e u_e$) and F_w^* is a shear function. These functions are in the transformed plane and must be converted for use in the physical plane. Dewey [22] has shown that in the physical plane using an intrinsic coordinate system the streamwise distance function can be represented by

$$S^* = 0.4863 \left(\frac{\nu_e x}{u_e \theta_0^2}\right) \tag{2.30}$$

which can be rewritten in terms of the Reynolds number, R_{e_x}, as

$$S^* = 0.4863 \left(\frac{x^2}{R_{e_x} \theta_0^2}\right) \quad , \tag{2.31}$$

where θ_0 represents the momentum thickness at the point of separation. Figure 7 shows the variation of the dividing streamline velocity as a function of the streamwise distance function S* as determined by Dennison and Baum. The nonfully developed dividing streamline velocity

required for the reattachment analysis was determined from a logarithmic curve fit of the data presented in this figure.

Equation (2.26) can be rewritten for the upper shear layer as

$$\eta_a = \frac{\delta_a \sqrt{R_{e_x}}}{x\sqrt{2}} \int_0^1 \frac{\rho_d}{\rho_\infty} d\zeta \quad , \tag{2.32}$$

which when integrated can be written as

$$\eta_a = \frac{\delta_a \sqrt{R_{e_x}}}{2\sqrt{2}\, x} \frac{1 - c_a^2}{c_d} \left[\ell n \frac{1 + c_d}{1 - c_d} \right] \quad . \tag{2.33}$$

Also,

$$\eta_b = \frac{\delta_a \sqrt{R_{e_x}}}{2\sqrt{2}\, x} \frac{\varphi_d}{\frac{\partial \varphi}{\partial \zeta}\Big|_d} \frac{\left(1 - c_a^2\right)}{c_d} \left[\ell n \frac{1 + c_d}{1 - c_d} \right] \quad . \tag{2.34}$$

In addition, the mixing ordinate can be defined as

$$\eta = \frac{\sigma_L y}{x} \quad , \tag{2.35}$$

which is the same as that for turbulent mixing with the change to the appropriate spread rate parameter σ. The equation used for the spread rate parameter is that used by Page and Dixon [23], i.e.,

$$\sigma_L = \frac{\sqrt{R_{e_x}}}{2\sqrt{\alpha}} \quad , \tag{2.36}$$

where α is a reference perturbation velocity factor, u_∞/u_R, and for this analysis is taken to be equal to 2 in accordance with the analysis of Nash [24].

From the exact solution for laminar mixing,

$$\left.\frac{\partial \varphi}{\partial \zeta}\right|_0 = \frac{\delta_a}{u_a}\left.\frac{\partial u}{\partial y}\right|_0 \quad . \tag{2.37}$$

But since

$$\left.\frac{\partial u}{\partial y}\right|_0 = \frac{u_d}{\delta_b} \quad ,$$

we have

$$\left.\frac{\partial \varphi}{\partial \zeta}\right|_0 = \frac{\delta_a}{\delta_b}\varphi_d \quad , \tag{2.38}$$

where

$$\varphi_d = \frac{u_d}{u_a} \quad .$$

The initial values required for the problem solution are obtained by calculating the value of the dividing streamline velocity from the curve fit, making an initial guess at the value of the parameter $\delta_a \sqrt{R_{e_x}}/x$, and then iterating the system of Eqs. (2.33), (2.34), and (2.38) until the system converges to within satisfactory accuracy. From this analysis, the initial values of δ_a, δ_b, φ_d, and the mixing integrals are determined for use in the reattachment part of the analysis.

2.3 Analysis for Redevelopment Region

The analysis for the redevelopment of the flow downstream of the reattachment point is carried out using basically the same techniques employed for the reattachment analysis. It is recognized that the characteristics of the flow will be the realignment of the external inviscid flow into the original horizontal direction. The initial

conditions required can be estimated from previous information obtained at the reattachment point. Figure 8 is a representation of the geometry and the modifications required to establish the starting conditions.

2.3.1 The Flow Condition at the Initial Section of Redevelopment

Immediately after the reattachment, the viscous flow undergoes a change until it reaches a section r' while the same free-stream condition prevails. A continuous rise in wall static pressure has been observed and it can only be made possible from a continuous transfer of mechanical energy to the dividing streamline (wall streamline). Thus, the curvature of the velocity profile at the wall plays a predominant role in this redevelopment process. The assumed velocity profile for the reattaching flow does possess such a built-in feature, namely that the curvature of the velocity profile at the wall is the largest when the transfer of energy is most needed ($\partial\varphi/\partial\zeta\,|_d = 0$). One may thus adopt the same velocity profile for the entire developing region ($\varphi_d = 0$).

It is then postulated that the velocity profile slope at the new section r' is determined from the condition that the same mass rate of flow passes through both sections r and r' as shown in Fig. 8.

From continuity principles, one may write

$$\int_0^{\delta_a} \rho u\,dy = \int_0^{\delta'_a} \rho u\,dy$$

or

$$\delta_a \int_0^1 \frac{\rho}{\rho_e} \varphi \, d\zeta \bigg|_r = \delta_a' \int_0^1 \frac{\rho}{\rho_e} \varphi \, d\zeta \bigg|_{r'} \quad . \qquad (2.39)$$

The geometric configuration gives the relationship

$$\delta_a' = \cos \theta_\infty \, \delta_a$$

Thus, Eq. (2.39) can be written

$$\int_0^1 \frac{\rho}{\rho_e} \varphi \, d\zeta \bigg|_r = \cos \theta_\infty \int_0^1 \frac{\rho}{\rho_e} \varphi \, d\zeta \bigg|_{r'} \quad . \qquad (2.40)$$

Using the assumed velocity distribution

$$\varphi = \frac{d\varphi}{d\zeta}\bigg|_0 \zeta + \left(3 - 2 \frac{d\varphi}{d\zeta}\bigg|_0\right)\zeta^2 + \left(\frac{d\varphi}{d\zeta}\bigg|_0 - 2\right)\zeta^3 \qquad (2.41)$$

at the section r', one may iterate on the slope $d\varphi/d\zeta\,|_0$ until the relationship given in Eq. (2.40) is satisfied.

The normal momentum conservation principle will be subsequently applied to determine the pressure level at r'. One recognizes that the momentum flux normal to the wall at the section is given by

$$\int_0^{\tilde{\delta}_a} \rho u \left(- u \sin \theta_\infty + v \cos \theta_\infty\right) dy$$

$$= - \rho_e u_e^2 \delta_a \int_0^1 \frac{\rho}{\rho_e} \varphi^2 \sin \theta_\infty \, d\zeta + \rho_e u_e^2 \delta_a \int_0^1 \frac{\rho}{\rho_e} \varphi^2 \cos \theta_\infty \tan \beta \, d\zeta \quad ,$$

where

$$\frac{u}{v} = \tan \beta = \tan \beta_e \left(2\zeta - \zeta^2\right)$$

or

$$\int_0^{\delta_a} \rho u \left(- u \sin \theta_\infty + v \cos \theta_\infty\right) dy$$

$$= - \rho_e u_e^2 \delta_a \left[\int_0^1 \frac{\rho}{\rho_e} \varphi^2 \left(\sin \theta_\infty - \cos \theta_\infty \tan \beta\right) d\zeta\right]_r \quad . \quad (2.42)$$

For the section r', one may write

$$\int_0^{\delta_a} \rho uv dy = \rho_e u_e^2 \delta_a' \int_0^1 \frac{\rho}{\rho_e} \varphi^2 \frac{u}{v} d\zeta$$

or

$$- \int_0^{\delta_a'} \rho uv dy = \rho_e u_e^2 \delta_a' \tan \beta_e \left[\int_0^1 \frac{\rho}{\rho_e} \varphi^2 \left(2\zeta - \zeta^2\right) d\zeta\right]_{r'} \quad . \quad (2.43)$$

For the purpose of simplicity, the terms within the brackets in Eqs. (2.42) and (2.43) will be represented as I_r and I_r', respectively. Neglecting the lateral shear stresses at sections r and r', the momentum equation is

$$\rho_e u_e^2 \left[\delta_a' \tan \beta_e I_r' + \delta_a I_r\right] = \frac{1}{2} \left(p_w' + p_d\right) \delta_a \sin \theta_\infty - \int_0^{\delta_a} p dy \sin \theta_\infty$$

$$\rho_e u_e^2 \left[\delta_a' \tan \beta_e I_r' + \delta_a I_r\right] = \frac{p_e}{2} \left(\frac{p_w'}{p_e} + \frac{p_d}{p_e}\right) \delta_a \sin \theta_\infty - p_e \sin \theta_\infty \delta_a \int_0^1 \frac{p}{p_e} d\zeta \ .$$

After some algebraic manipulations and integration of the last term, the previous equation becomes

$$\left(\frac{2\gamma}{\gamma - 1}\right) \frac{c_e^2}{1 - c_e^2} \left[\cot \theta_\infty \tan \beta_e \int_0^1 \frac{\rho}{\rho_e} \varphi^2 \left(2\zeta - \zeta^2\right) d\zeta \right.$$

$$\left. + \int_0^1 \frac{\rho}{\rho_e} \varphi^2 \left(1 - \cot \theta_\infty \tan \beta\right) d\zeta \right]$$

$$= \frac{1}{8} \frac{p_w}{p_e} - \frac{1}{2} \frac{p'_w}{p_e} - \frac{5}{8} \quad . \tag{2.44}$$

This equation allows the evaluation of the wall pressure, p'_w/p_e, at section r'.

2.3.2. Downstream Redevelopment Flow

Once the flow properties at section x' have been established, it is simple to see that the downstream flow redevelopment involves the continued adjustment of the free stream toward the horizontal flow direction and the analysis suggested for the upper viscous layer in the preceding reattaching flows may readily be adopted for this rehabilitation process. The two equations already derived in Section (2.2.1) are rewritten for the new system of coordinates pertaining to this redeveloping flow region as

$$\tan \epsilon_e = \frac{u_e}{v_e} = \frac{d}{dx} \delta_a \int_0^1 \left(1 - \frac{\rho}{\rho_e} \varphi\right) d\zeta - \frac{\delta_a \int_0^1 \frac{\rho}{\rho_e} \varphi \, d\zeta}{\left(1 - c_e^2\right)^{\frac{1}{(\gamma - 1)}} c_e} \frac{d}{dx} \left(1 - c_e^2\right)^{\frac{1}{\gamma - 1}} c_e \quad .$$

(2.45)

$$\frac{\tau_w}{p_\infty u_\infty^2}\left(1 - c_\infty^2\right)^{\frac{1}{\gamma-1}} c_\infty^2 = \frac{d}{dx}\left[\left(1 - c_e^2\right)^{\frac{1}{\gamma-1}} c_e^2 \delta_a \int_0^1 \frac{\rho}{\rho_e}\varphi(1-\varphi)\, d\zeta\right]$$

$$+ \left(1 - c_e^2\right)^{\frac{1}{\gamma-1}} c_e \delta_a \left[\int_0^1 \left(1 - \frac{\rho}{\rho_e}\varphi\right) d\zeta\right] \frac{d c_e}{dx}$$

$$- \frac{3}{16}\left(\frac{\gamma-1}{\gamma}\right)\frac{d}{dx}\left[\left(1 - c_e^2\right)^{\frac{\gamma}{\gamma-1}} \delta_a \left(\frac{p_w}{p_e} - 1\right)\right] \quad , \qquad (2.46)$$

where $\epsilon_e = \omega(c_1) - \omega(c_e)$ and is negative throughout this region.

One important feature which is associated with this flow redevelopment can be discussed in detail as follows. During this flow redevelopment, the free stream adjusts itself continuously toward the horizontal flow direction thereby inducing an appreciable difference in the static pressure across the viscous layer. On the other hand, the low energy viscous layer close to the wall has to receive an adequate amount of mechanical energy to cope with the rise in pressure and this transfer is properly represented by the curvature of the velocity profile at the wall. It would seem to be advantageous to suggest that this curvature shall be proportional to the normal pressure difference, i.e.,

$$\left.\frac{\partial^2 \varphi}{\partial \zeta^2}\right|_0 = \left(3 - 2\left.\frac{d\varphi}{d\zeta}\right|_0\right)_{r'} = k\left(\frac{p_w'}{p_e} - 1\right) \quad , \qquad (2.47)$$

again with the value of k evaluated at the section r'. This arrangement would insure that the condition of a completely rehabilitated or relaxed state is reached far downstream.

According to Eq. (2.11), the normal pressure gradient for this region can be rewritten as

$$\frac{p_w}{p_e} = 1 + \frac{2\gamma}{\gamma - 1}\left\{\frac{c_e^2}{1 - c_e^2}\left[\tan^2 \epsilon_e - \tan \epsilon_e \frac{d\,\delta_a}{dx}\right]\right.$$

$$\left. + \frac{1}{\left(1 - c_e^2\right)^{\frac{1}{(\gamma - 1)}}} \frac{d}{dx}\left[\left(1 - c_e^2\right)^{\frac{1}{\gamma - 1}} c_e^2 \delta \int_0^1 \frac{\rho}{\rho_e} \varphi^2 \tan \beta \, d\zeta\right]\right\} . \quad (2.48)$$

To evaluate the wall shear stress term in Eq. (2.46), it is easy to see that

$$\tau_w = \mu \left.\frac{\partial u}{\partial y}\right|_w = \frac{\mu_w}{\mu_\infty} \mu_\infty \frac{u_e}{\delta_a} \left.\frac{\partial \varphi}{\partial \zeta}\right|_0$$

and one may obtain

$$\frac{\tau_w}{\rho_\infty u_\infty^2} \left(1 - c_\infty^2\right)^{\frac{1}{\gamma - 1}} c_\infty^2 = \left(1 - c_\infty^2\right)^{\frac{2 - \gamma}{\gamma - 1}} \frac{c_e c_\infty}{R_{e_\ell}} \frac{\ell}{\delta_a} \left.\frac{\partial \varphi}{\partial \zeta}\right|_0 , \quad (2.49)$$

where the linear viscosity-temperature relationship

$$\frac{\mu_w}{\mu_\infty} = \frac{T_0}{T_\infty}$$

has been employed.

3. CALCULATION METHOD AND RESULTS

3.1 Calculation Procedures

For a specific flow condition where the free-stream Mach number M_∞ and the boundary layer approaching the base are given (the boundary layer can usually be calculated from R_{e_ℓ}), one may select the base pressure ratio p_b/p_1 and the length ℓ_m along the wake boundary where recompression begins. The initial values required to calculate the recompression process may be determined by using the method outlined in Section 2.2.3. One now starts to integrate the system of differential equations for the reattachment region. At each increment of length along the dividing streamline, values for the free-stream Crocco number c_e and the dividing streamline velocity φ_d are selected and iterated upon until the system of equations is satisfied. For each set of these values, δ_a may be found from Eq. (2.2), p_d/p_e from Eq. (2.11), δ_b from Eq. (2.15), p_w/p_d from Eq. (2.18), h_b from Eq. (2.16), and c_b from Eq. (2.14). Using this information, one obtains two residues from Eqs. (2.7) and (2.23). The values for c_e and φ_d at this location are iterated upon until the residues become negligible.

The above calculations are continued until the stagnation point is reached. At this point φ_d is set to zero and the wall pressure now becomes the stagnation pressure of both the dividing streamline and the back flow. Using the normal momentum relationship given by Eq. (2.18), the correct value of the free-stream Crocco number at the stagnation

point can be determined when the wall pressure is obtained from the averaging of previously determined curves for p_{0_d} and p_{0_b}. Once again, two residues are obtained at the rear stagnation point. These are the residues for the whole set of calculations. One now iterates upon the initially selected values for base pressure ratio p_b/p_1 and the location ℓ_m for the starting of the recompression process until the residues at the stagnation point becomes vanishingly small. This establishes the correct flow field up to this point.

From the preceding calculations one has available the initial values needed for calculating the flow field redevelopment downstream of the reattachment point. Using Eqs. (2.44), the value for the wall pressure ratio p_w/p_1 is determined for the section r'. Then Eqs. (2.45), (2.46), and (2.47) are solved together. The values of c_e is to be iterated upon until the residue from Eq. (2.46) is reduced to zero. The calculation proceeds downstream until the flow angle calculated by Eq. (2.45) becomes zero. At this point the value for the wall pressure ratio p_w/p_1 should be equal to 1.

It should be noted that the method of calculation used for the reattachment analysis exhibits the typical elliptical behavior of separated flow problems. A unique value of the base pressure ratio is determined using this scheme of calculation up to the reattachment point. In all of the calculations the influence of this pressure variations across the upper layer on to the density was neglected and the density was estimated as if the viscous layer had the constant free-stream pressure, i.e.,

$$\frac{\rho}{\rho_e} = \frac{\left(1 - c_e^2\right)}{\left(1 - c_e^2\, \varphi^2\right)}$$

In addition, the lateral shear stress terms have been neglected in the estimation of the pressure differences across the layers since their contribution was found to be indeed small.

3.2 Results of Calculations

Figure 9 shows a comparison between the calculated and experimental wall pressure ratio p_w/p_1 as a function of downstream distance from the step for a free-stream Mach number of 2.0 and a Reynolds number, based upon the characteristic length ℓ from the leading edge of the plate to the point of separation, of 170,000 [25]. The calculated base pressure value of 0.680 compares very favorably with the experimental value of 0.670; in fact, this represents an error of only approximately 2 percent. The pressure rise in the recompression region is steeper for the theoretical solution than that for the experimental data but the overall comparison looks satisfactory. The corresponding velocity and stagnation pressure ratios for this case are shown in Figs. 10 and 11.

It is pertinent to mention that other research activities on separated flow conducted at the University of Illinois [26] indicated that the point of reattachment clearly exhibits itself as a saddle point for the governing system of equations. This fact implies that the present calculations may predict accurately the base pressure but not the flow properties in the vicinity of the point of reattachment. Indeed, if one continued the calculations for the redevelopment region for the flow case presented in Fig. 9, the wall pressure ratio would not have agreed with the experimental data within that region. Adjustments in the thickness of the viscous layer and the free-stream Mach number have been made at the point of reattachment such that the

calculated results agreed favorably with the experimental data. This does indicate that the scheme of analysis for the flow rehabilitation downstream of the reattachment would describe the flow events correctly if the conditions at the point of reattachment were accurately determined.

One of the ways to assess the validity of a particular analytical method is to assess its application at several different Mach numbers. Some difficulty was noted when the proposed method was applied for flows with higher Mach numbers. The base pressure ratio correlated very well with experimental data [27] over a wide Reynolds number range at a Mach number of 2.5 as shown in Fig. 12; however, the wall pressure ratio rise within the reattachment region did not agree at all. Again, this perhaps shows the saddle point behavior of the reattachment point. Other factors which could have caused such a discrepancy will be discussed later. The excellent correlation, however, for the base pressure ratio over the large Reynolds number range further substantiates the fact that a unique solution for the base pressure is obtained from the solution of the integral equations.

Figure 13 shows the calculated wall shear stress downstream of the reattachment point. The distribution appears to follow the expected trend beginning with zero at the stagnation point, rising to a plateau level thereafter. After the flow reaches the fully rehabilitated state, it is expected that the wall shear stress will decrease toward zero asymptotically far downstream. This is well borne out from the analysis since $\partial\varphi/\partial\zeta|_0$ reaches a constant value of 3/2 far downstream. For comparison purposes, the variation of the shear stress coefficient for the equivalent flat plate flow, when the effect of the

back step is disregarded, is also shown i. Fig. 13. This curve serves to indicate the correct level of the plateau obtained from the shear stress calculations.

4. DISCUSSION AND CONCLUSIONS

The reattachment and subsequent redevelopment for laminar supersonic flow over a back step can be calculated using the described procedure. The calculated results compare favorably for one particular Mach number while yielding a generally unsatisfactory pressure distribution at a higher Mach number. Several reasons for this disagreement are apparent. First of all, it is difficult to evaluate or to completely satisfy one's self that the experimental data are for completely laminar flow even though the Reynolds numbers are low. In fact, if the flow is transitional, one would expect the pressure gradient and the reattachment point to occur closer to the base than that for laminar flow and this is the case for the data used at Mach number 2.5. Additionally, one may expect that as the Mach number is increased, disregarding the rotational flow field interacting with the upper viscous layer might have caused a sizable error in the estimation of the initial conditions required for the reattachment calculations. This effect was recognized in the latter part of this investigation. It is suggested that future research studies should take this effect into consideration.

The method chosen for the redevelopment region has been shown to yield satisfactory results. Accounting for the wall shear stress made little difference in the wall pressure ratios. This probably was due to the exceedingly small magnitude of the calculated shear stress values.

Additionally, it was also determined through sample calculations that the inclusion of the lateral shear stress in the estimation of the pressure difference across the viscous layer made essentially no change in the magnitude of the base pressure and the distribution of the wall pressure ratio. This fully justifies the original approach to disregard their contribution.

Finally, it should be noted that this suggested flow model can be used for other separated flow problems. Similar models can be developed for low speed flow and the analysis can also be extended to axisymmetrical configurations.

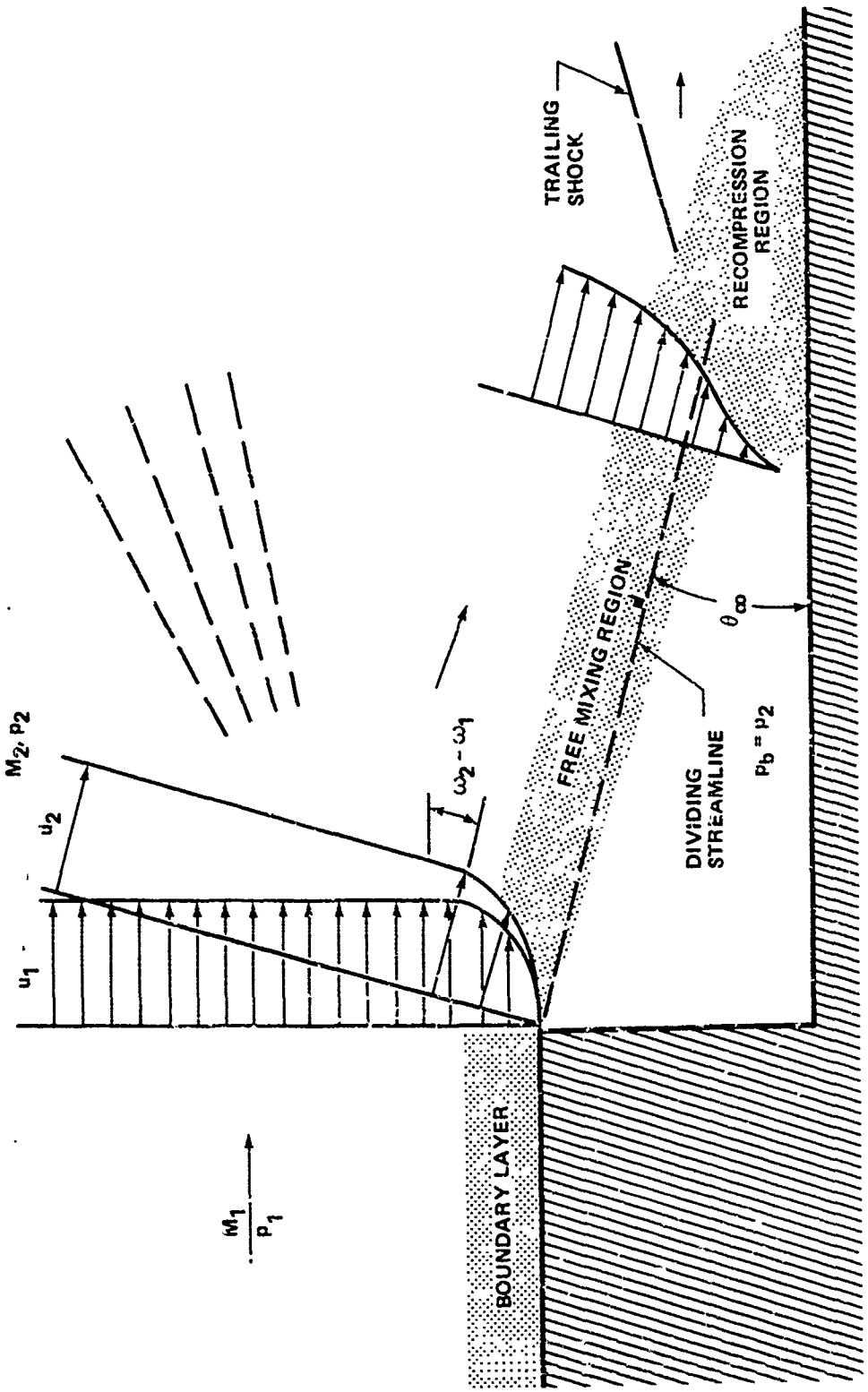

Figure 1. Two-Dimensional Supersonic Flow Past a Back Step

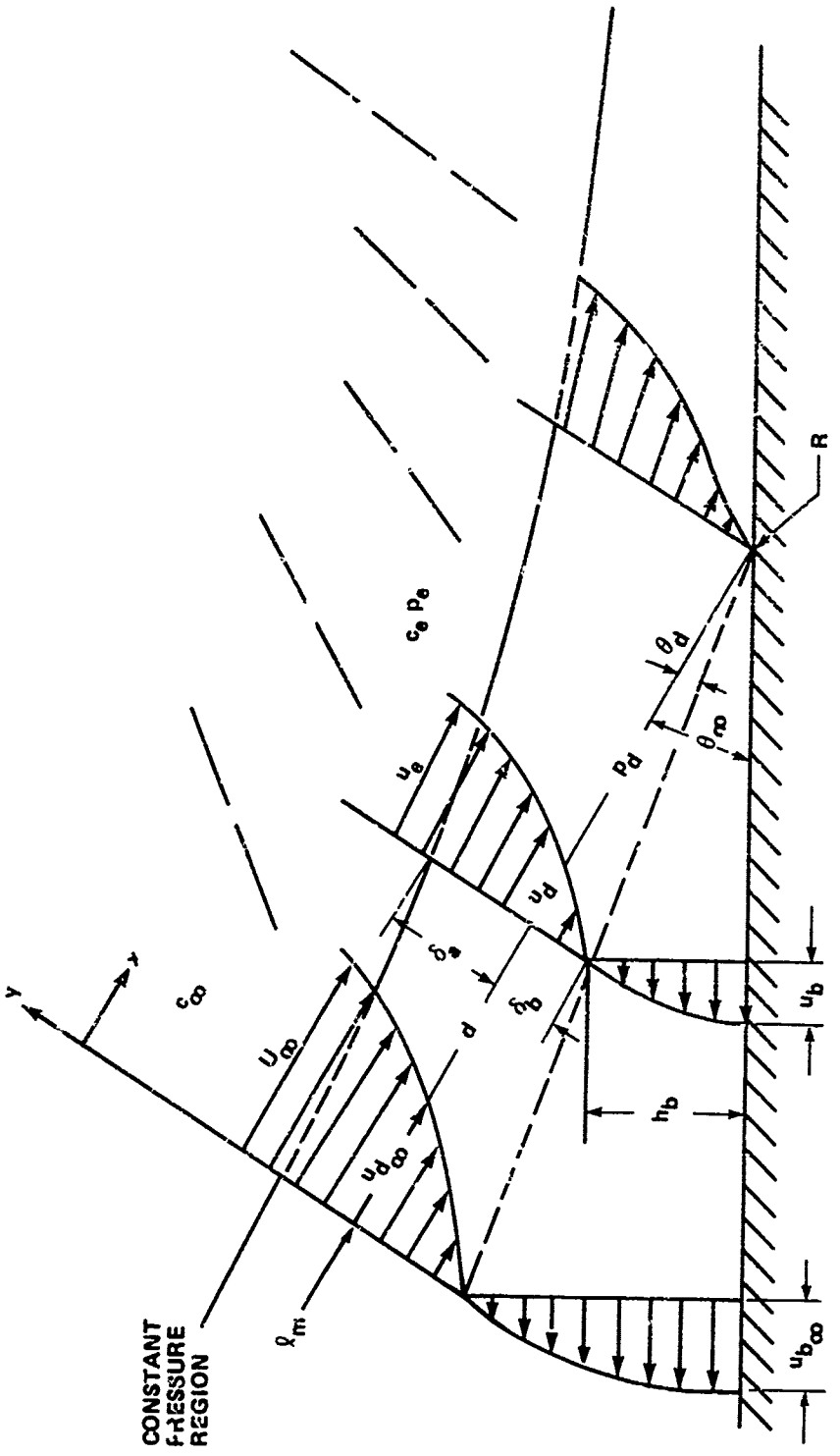

Figure 2. The Flow Model for Recompression Study

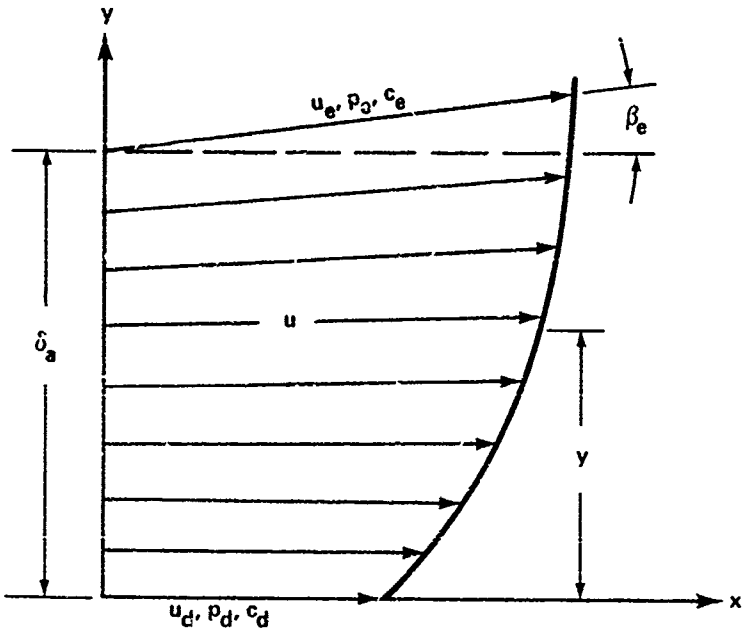

Figure 3. The Upper Shear Layer

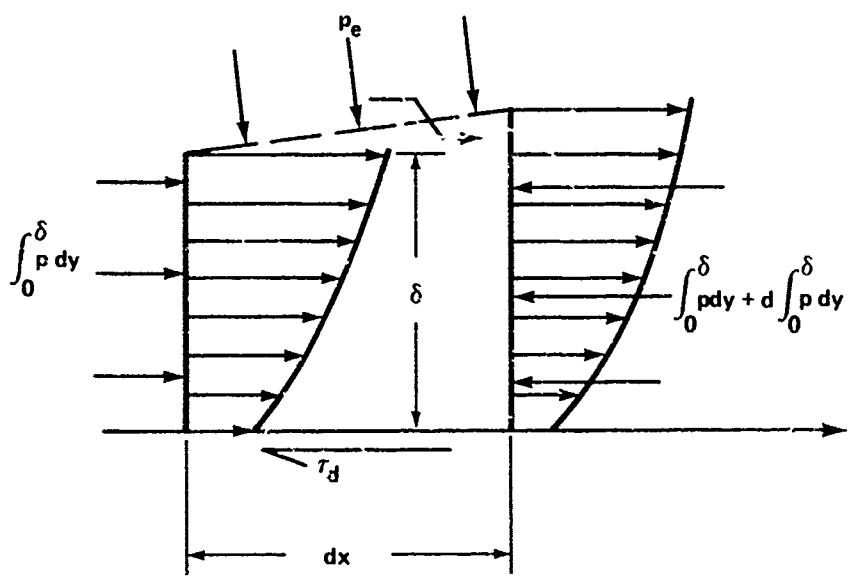

Figure 4. Elementary Control Volume for Upper Viscous Layer

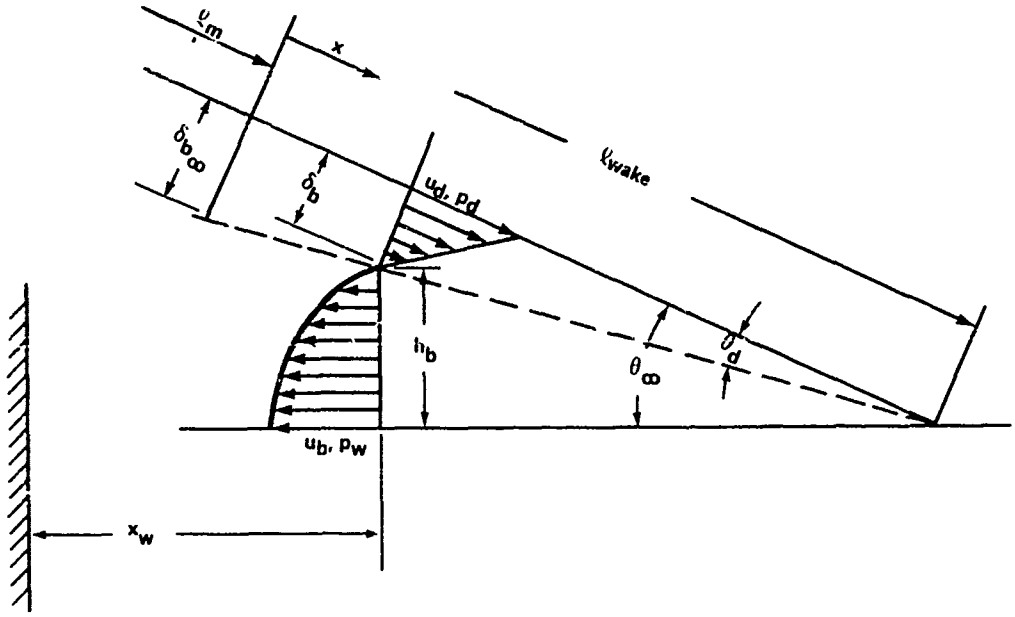

Figure 5. The Lower Shear Flow Region

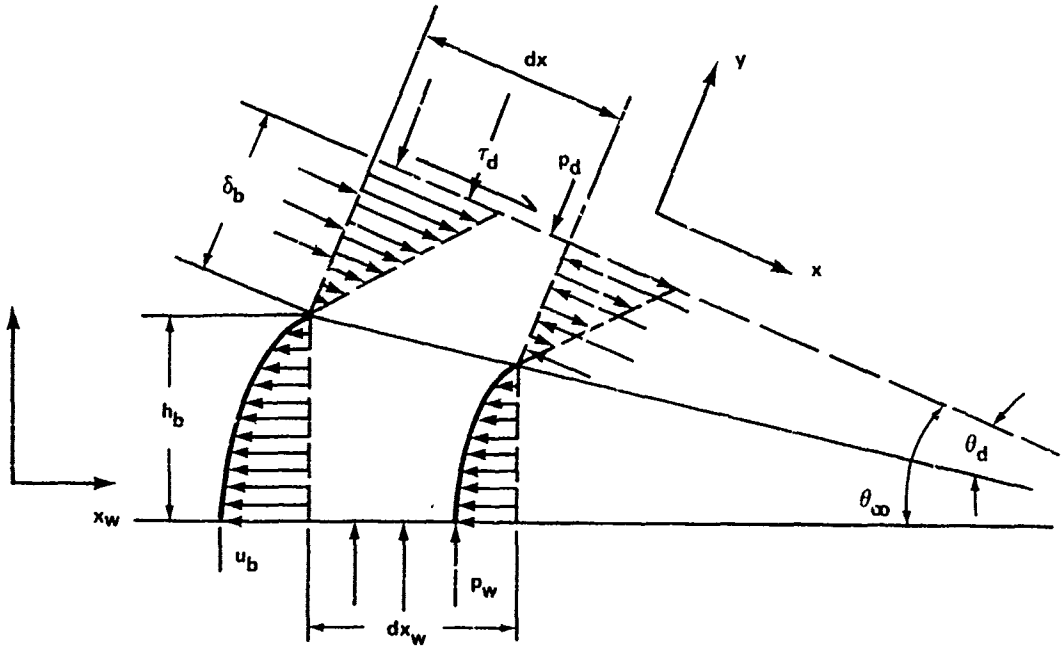

Figure 6. Elementary Control Volume for Lower Viscous Flow Region

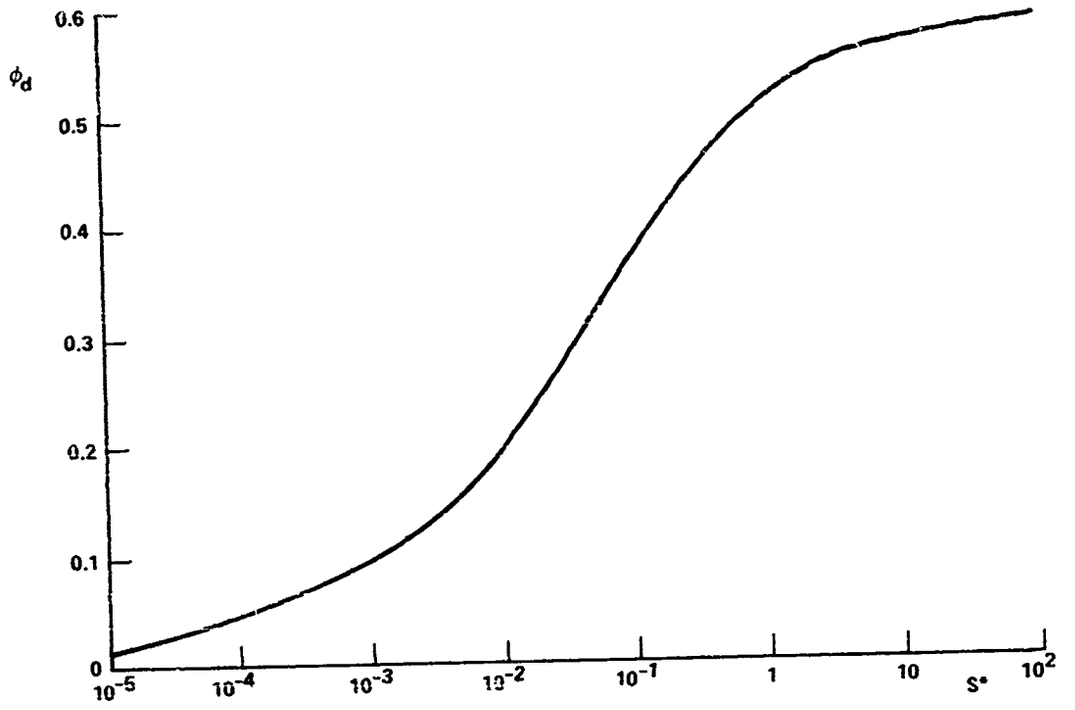

Figure 7. Velocity of the Dividing Streamline [21]

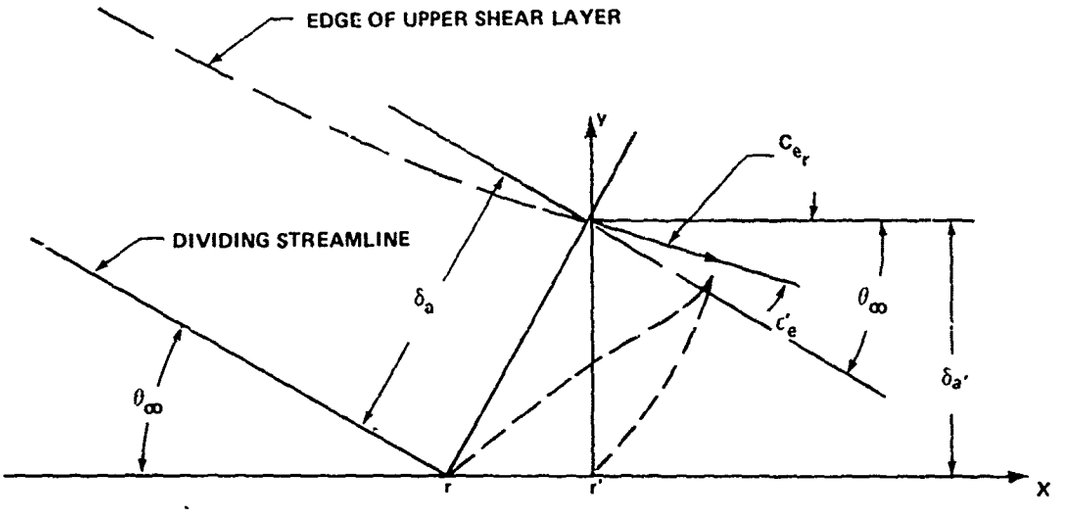

Figure 8. Redevelopment Flow Field

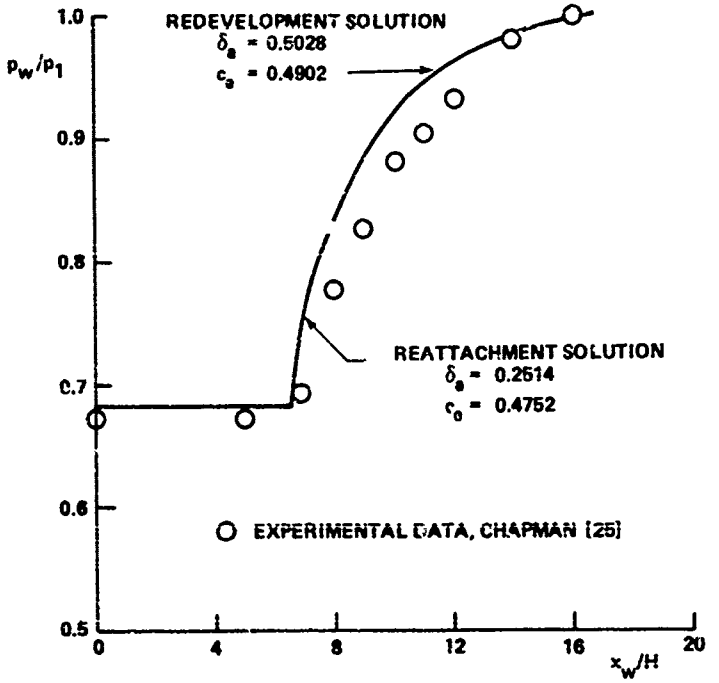

Figure 9. Theoretical and Experimental Wall Pressure Distribution for $M_1 = 2.0$, $R_{e_\ell} = 170{,}000$

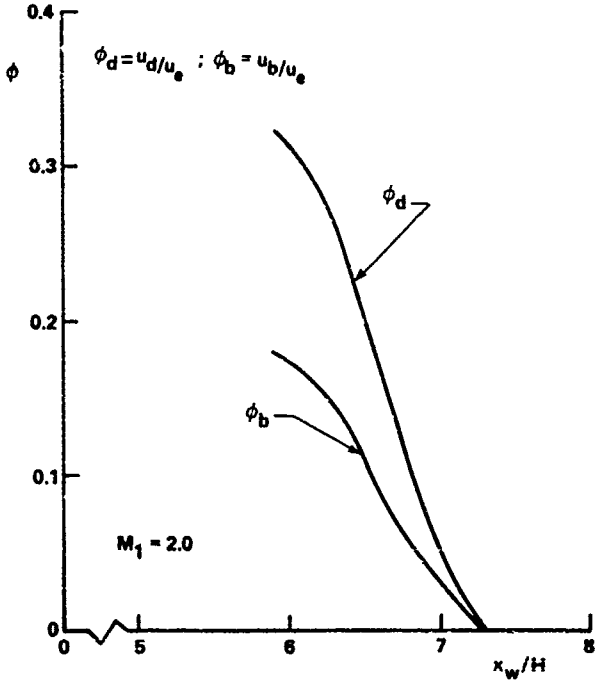

Figure 10. Variation of Velocity Ratios for $M_1 = 2.0$, $R_{e_\ell} = 170{,}000$

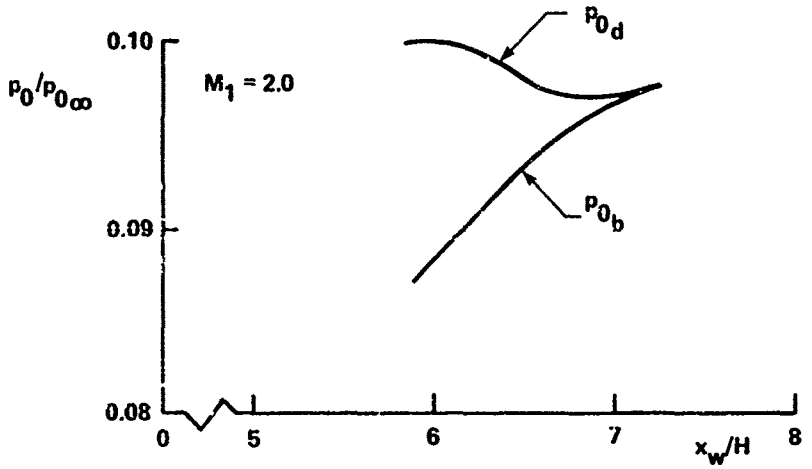

Figure 11. Variation of Stagnation Pressure Ratios for $M_1 = 2.0$, $R_{e_\ell} = 170{,}000$

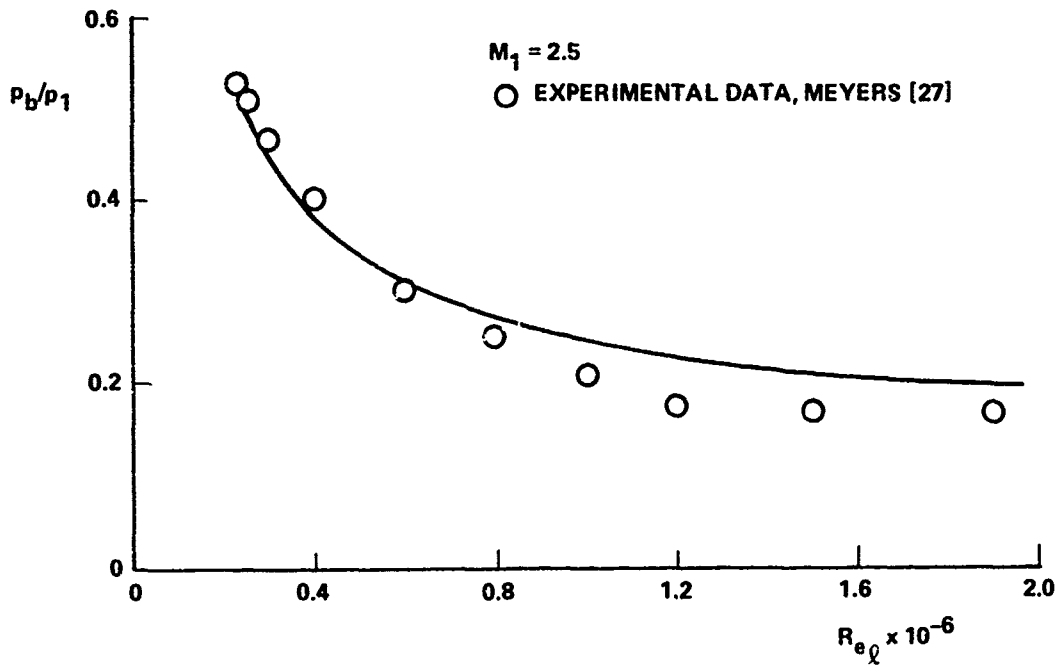

Figure 12. Variation of Base Pressure with Reynolds Number for $M_1 = 2.5$

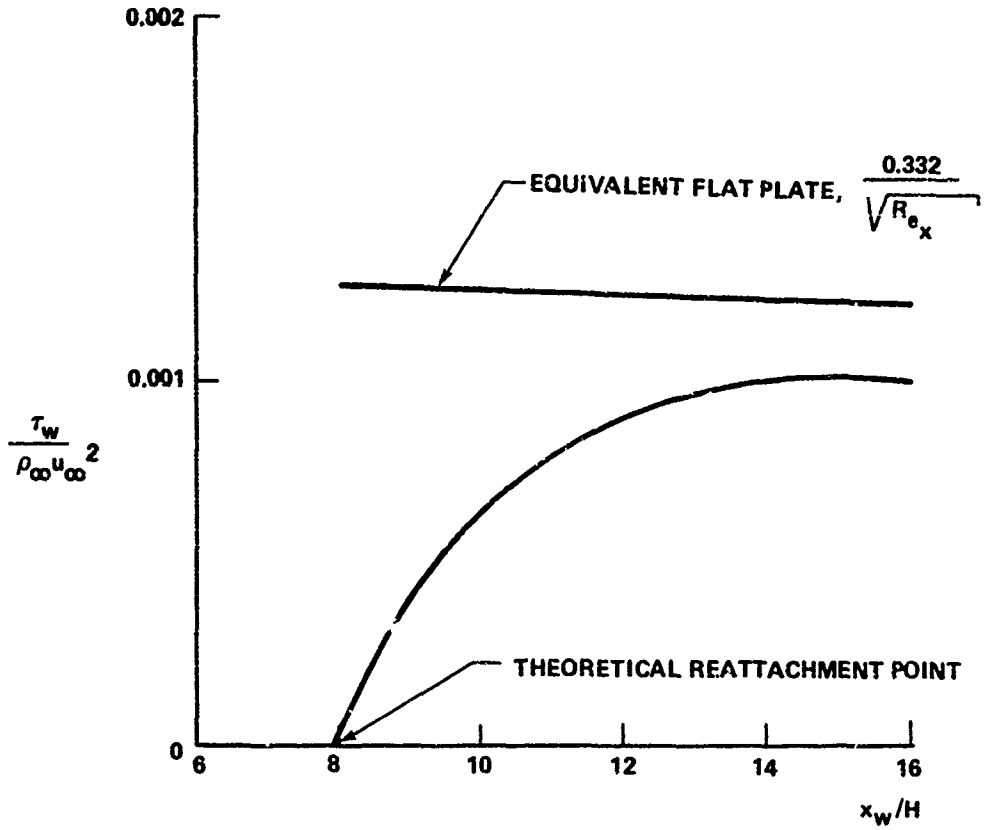

Figure 13. Variation of Wall Shear Stress in Redevelopment Region for $M_1 = 2.0$, $R_{e_\ell} = 170{,}000$

REFERENCES

1. Gabeaud, A., "Base Pressures at Supersonic Velocities," Journal of Aerospace Sciences, Vol. 17, No. 8, August 1950.

2. von Karman, T. and Moore, N. B., "Resistance of Slender Bodies Moving with Supersonic Velocities, with Special Reference to Projectiles," Transactions American Society of Mechanical Engineering, Vol. 54, 1932, p. 302.

3. Hill, F. K., "Base Pressures at Supersonic Velocities," Journal of Aerospace Sciences, Vol. 17, No. 3, March 1950, p. 185.

4. Chapman, D. R., "An Analysis of Base Pressure at Supersonic Velocities and Comparison with Experiment," NACA TN-2137, 1950.

5. Love, E. S., "Base Pressure at Supersonic Speeds on Two-Dimensional Airfoils and on Bodies of Revolution With and Without Fins Having Turbulent Boundary Layers," NACA TN-3819, 1957.

6. Crocco, L. and Lees, L., "A Mixing Theory for the Interaction Between Dissapative Flows and Nearly Isentropic Streams," Journal of Aerospace Sciences, Vol. 19, No. 10, October 1952, pp. 649-476.

7. Chapman, D. R., "Analysis of Base Pressures at Supersonic Velocities and Comparison with Experiment," NACA Report 1051, 1951.

8. Korst, H. H., "A Theory for Base Pressures in Transonic and Supersonic Flow," Journal of Applied Mechanics, Vol. 23, 1956, pp. 593-600.

9. Chapman, D. R., "Laminar Mixing of a Compressible Fluid," NACA Report 958, 1950, (Formerly NACA TN-1800).

10. Lees, L. and Reeves, B. L., "Supersonic Separated and Reattaching Laminar Flows: 1. General Theory and Application to Adiabatic Boundary Layer - Shock Wave Interactions," AIAA Journal, Vol. 2, 1964, pp. 1907-1920.

11. Reeves, B. L. and Lees, L., "Theory of Laminar Near Wake of Blunt Bodies in Hypersonic Flow," AIAA Journal, Vol. 3, 1965, pp. 2061-2074.

12. Alber, I. E. and Lees, L., "Integral Theory for Supersonic Turbulent Base Flows," AIAA Journal, Vol. 6, 1968, pp. 1343-1351.

13. Nash, J. F., "An Analysis of Two-Dimensional Turbulent Base Flow," Including the Effect of the Approaching Boundary Layer, Aeronautical Research Council R. and M. No. 3344, July 1962.

14. Crawford, D. R., "Supersonic Separated Flow Downstream of a Backward Facing Step," Ph.D. Thesis, University of California, Berkeley, May 1967.

15. Roadie, P. J. and Mueller, T. J., "Numerical Solutions of Laminar Separated Flows," AIAA Journal, Vol. 8, 1970, pp. 530-538.

16. Weiss, R. F. and Weinbaum, S., "Hypersonic Boundary-Layer Separation and the Base Flow Problem," AIAA Journal, Vol. 4, 1966, pp. 1321-1330.

17. Weiss, R. F., "Base Pressure of Slender Bodies in Laminar Hypersonic Flow," AIAA Journal, Vol. 4, 1966, pp. 1557-1559.

18. Weiss, R. F., "A New Theoretical Solution of the Laminar Hypersonic Near Wake," AIAA Journal, Vol. 5, 1967, pp. 2142-2149.

19. Weinbaum, S., "Rapid Expansion of a Supersonic Boundary Layer and Its Application to the Near Wake," AIAA Journal, Vol. 4, 1966, pp. 217-226.

20. Chow, W. L., "Recompression of a Two-Dimensional Supersonic Turbulent Free Shear Layer," Developments in Mechanics, Vol. 6, Proceedings of the 12th Midwestern Mechanics Conference, 1970, pp. 319-331.

21. Denison, M. R. and Baum, E., "Compressible Free Shear Layer with Finite Initial Thickness," AIAA Journal, Vol. 1, 1963, pp. 342-349.

22. Dewey, C. F., Jr., "Measurements in Highly Dissipative Regions of Hypersonic Flows. Part II. The Near Wake of a Blunt Body at Hypersonic Speeds," Ph.D. Thesis, California Institute of Technology, 1963.

23. Page, R. H. and Dixon, R. J., "A Transformation for Wake Analysis," AIAA Journal, Vol. 2, No. 8, 1964, pp. 1464-1465.

24. Nash, J. F., "Laminar Mixing of a Non-Uniform Stream with a Fluid at Rest," Aeronautical Research Council Report 22245, F. M. 3005, September 1960.

25. Chapman, D. R., Kuehn, D. M., and Larson, H. K.; "Investigation of Separated Flows in Supersonic and Subsonic Streams with Emphasis on the Effect of Transition," NACA Report 1356, 1958.

26. Chow, W. L., "Fluid Dynamics and Heat Transfer Problems of Modern Air Breathing Propulsive Systems," Progress Report QSR-8, prepared for NASA Research Grant NGL 14-005-140, Department of Mechanical and Industrial Engineering, University of Illinois at Urbana-Champaign, July 1971.

27. Meyers, A. W., "A Survey of Rearward-Facing Steps in Two-Dimensional Supersonic Flow," Masters Thesis, University of Tennessee, 1967.